A Computational Model of the Trans-Synaptic Spread of Pathogenic Tau in Early Alzheimer's Disease

***Bashir Sbaiti[1,3], *Michael Khalfin[2,3], Marianne Bezaire[3,4]**
[1]Cumberland Valley High School, Mechanicsburg, Pennsylvania 17050; [2]Plainview-Old Bethpage JFK High School, Plainview, New York 11803; [3]Boston University RISE Program, Boston, Massachusetts 02215, [4]Psychological & Brain Sciences, Boston University, Boston, Massachusetts 02215
**Authors had an equal contribution to the work*

Alzheimer's Disease is an extremely prevalent neurodegenerative disorder which causes progressive cognitive decline. This disease is associated with the spread of pathogenic tau protein, which starts in the transentorhinal cortex and progresses to other limbic and cortical areas. Tau is an important structural protein that stabilizes neuronal microtubules. In Alzheimer's Disease, pathogenic tau proteins detach from microtubules and form neurofibrillary tangles, inhibiting normal neuronal function. Pathogenic tau can spread between neurons via synaptic transmission, so leading therapeutics target its pathological isoforms and inhibit their uptake into adjacent cells. We report the development of a tau propagation computational model based on neuronal firing rates that simulates protein removal as the result of therapeutic intervention and describes its net effects on a neuronal network. Using this model, the tau prevalence and cell death over time were measured to assess a simulated therapeutic's efficacy. For a quick and efficient alternative method that predicts drug efficacy without running the full simulation, we also trained a machine learning algorithm called a polynomial support vector machine, which classifies a drug's efficacy given its parameter values. Our data suggest that the most effective therapeutic solutions must affect 95% of infected cells and reduce their tau spreading activity by 85% in order to maintain a 99% neuronal survival rate. Through statistical analysis, we also concluded that targeting a greater tau population is more important than reducing tau by a greater factor to impair tau spread for the most effective therapeutics. Such findings have the potential to guide the development and administration of therapeutics. The simulation itself can also allow future investigators to gain a better understanding of how different factors (i.e. cell type, connectivity) affect tau propagation in AD.

Abbreviations: AD – Alzheimer's Disease; NFTs – neurofibrillary tangles; SVM – support vector machine

Keywords: Neurodegenerative disease; tauopathy; tau propagation; small-world network; therapeutic intervention; tau reduction

Introduction

Alzheimer's Disease (AD) is a neurodegenerative disorder that impacts approximately 6.2 million Americans per year (Alzheimer's Association, 2021). By 2050, this number is projected to grow to 13.8 million (Alzheimer's Association, 2019). AD is the leading source of dementia among older individuals, and its pathology is associated with tau protein misfolding (Cortes-Canteli and Iadecola, 2019). In healthy neurons, soluble tau is involved in the structural polymerization and stabilization of microtubules; but protein hyperphosphorylation leads to conformational changes that trigger tau's detachment from microtubules (Iqbal et al., 1986). The free-floating tau then aggregates within neurons in inert structures called neurofibrillary tangles (NFTs) (Hyman, 1997). At this point, the tau

protein becomes a prion, or a transmissible pathogenic agent (Stopschinski and Diamond, 2017; Colin et al., 2020).

It is important to study tau pathology because it is not only relevant in AD, but also in many other diseases such as progressive supranuclear palsy and Pick's disease (Williams, 2006). Furthermore, studying tau pathology can reveal properties of other prions, such as prions that are characteristic of Parkinson's disease (α-synuclein), Huntington's disease (mutant huntingtin), or amyotrophic lateral sclerosis (superoxide dismutase 1) (Stopschinski and Diamond, 2017).

During prodromal (early) AD, tau pathology begins in the transentorhinal cortex, located adjacent to the entorhinal and hippocampal regions within the medial temporal lobe (Taylor and Probst, 2008). In AD, adjacent brain regions are gradually impacted (Braak and Braak, 1991; Vogel et al., 2020). As the disease worsens, tau spreads to the proper entorhinal cortex, Ammon's horn sector, and eventually the entire association neocortex (Braak and Braak, 1995; Serrano-Pozo et al., 2011). The leading hypothesis describes this phenomenon as tau propagation and claims that interneuronal transfer of tau is responsible for progressive neurodegeneration (Takeda, 2019). First, tau is released from the presynaptic cell into the extracellular environment by passive or active release at the synaptic cleft (Yamada et al., 2014). Then, a seed tau traverses the synapse and is assimilated by the postsynaptic cell via endocytosis (Frost et al., 2009). Alternatively, neurons can release exosomes which transport tau (Wang et al., 2017). Pathological tau creates an inevitable cascading effect which precipitates cell death via the impairment of microtubular function (Iqbal et al., 2010).

In AD, targeted therapeutic intervention can remove extracellular tau and halt the process of cognitive decline (Nobuhara et al., 2017; Nicholls et al., 2017). Molecular biologists have conducted experiments to determine binding affinities for tau at different epitopes (Nobuhara et al., 2017). Additionally, because tau conforms to multiple isoforms, research is being done to determine which manifestations of the protein lend themselves to AD pathological defects (Luna-Munoz et al., 2007; Adams et al., 2010). Until the binding affinities for different sites on the protein and the toxicity of tau's isoforms are better understood, pharmaceutical intervention will remain challenging (Iqbal et al., 2010). Still, experimental therapeutics including the murine versions of BIIB076 and UCB0107 have successfully combated tau propagation *in vitro* (Nobuhara et al., 2017; Courade et al., 2018). They use the isotype Immunoglobulin G4 which can lower extracellular excitotoxicity and limit cell internalization of tau (Courade et al., 2018). While some compounds have been shown to effectively slow the spread of tau, AD research would benefit from a model that specifically explains therapeutics' impact on tau propagation.

In the present study, we investigated which characteristics of a potential therapeutic are most crucial in their ability to limit tau spread and resulting cell death by developing and executing an *in silico* model of tau propagation in early AD, originating in the transentorhinal cortex. In the model, transentorhinal cortical connectivity is approximated by a Watts-Strogatz small-world network because such networks exhibit physiologically realistic traits such as high clustering and low mean path length (Watts, 1999; Yang, 2013).

Our first hypothesis was that different network properties of therapeutics can influence their efficacy to varying extents. More specifically, we hypothesized that in order for a therapeutic to be maximally effective, it must primarily affect a large proportion of neurons in a network, and the amount by which pathogenic tau is reduced within each neuron is less important but still varies proportionally with therapeutic efficacy. This is because the highly interconnected network nature of the brain means that tau propagation will quickly increase to an uncontrollable rate, so pervasive rather than potent therapeutics may be the most effective (Braak and Braak, 1991; Vogel et al., 2020).

Additionally, we aimed to apply an SVM (support vector machine) algorithm to analyze the resulting data gathered via *in silico* simulations, with the goal of accelerating the process of evaluating therapeutic efficacy. An SVM is a supervised machine learning algorithm that can be used to solve classification problems (Noble, 2006). The algorithm draws decision boundaries around training data points on a graph, grouping

them according to their class (Vishwanathan and Murty, 2002). It is useful in neuroscience because of its affinity for deducing patterns from training sets (Pisner and Schnyer, 2020). As such, our second hypothesis was that an SVM algorithm trained on simulation data could predict an anti-tau therapeutic's efficacy significantly faster than running the full *in silico* simulation in certain scenarios.

Methods

Network Generation

Transentorhinal cortical connectivity was approximated using a Watts-Strogatz small-world network modified such that connections were non-symmetrical and directed (Watts and Strogatz, 1998).

Table 1: Network Parameters

Symbol	Description
N	Number of nodes
k	Number of connected neighbors in a ring topology
P	Probability of replacing a connection to a neighbor with a connection to another node

Note. The symbol and description of each of the three parameters with which the network was created.

For N = 1000 and k = 20, values of P were investigated to maximize the mean clustering coefficient and minimize the mean path length. This set of parameters specified a network with 1000 neurons, each connected to 20 other neurons in the network. Python (version 3.8, Spyder 4 IDE) module NetworkX was used to gather appropriate network statistics.

Figure 1 is a graphical representation of the mean clustering coefficient and mean path length at various values of P. Through analysis of Figure 1, P = 0.05 appeared to be the optimal value for generating a network that fit the required specifications (high clustering and low

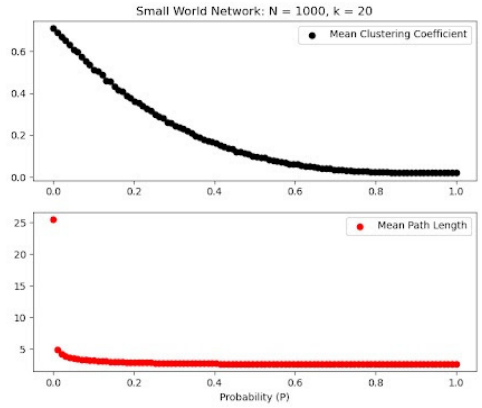

Figure 1: These plots were produced by performing a parameter scan of 100 values of probability P between 0.0 and 1.0. The Probability (P) is on the x-axis and the y-axis represents mean clustering length (top) as well as mean path length (bottom).

path length). To better understand the network, a function to visualize it in a ring topology was created (Figure 2). The graphical representation confirmed that each node had an expected amount of random connections so as to resemble a biologically realistic small-world network, but not unlimited connections on the order of a scale-free network (Warren et al., 2002). Also, another function was created to display the network as a gridlike adjacency matrix (Figure 3). The visualization showed that clustering occurred across a diagonal, which was desired during the creation of the network (Watts and Strogatz, 1998). The figure was additionally important because it directly contributed to the model code.

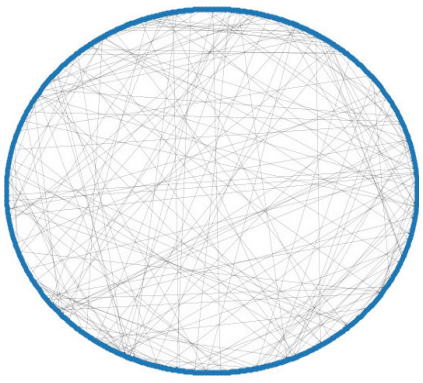

Figure 2: The ring topology of the network, showing all nodes and the edges connecting them.

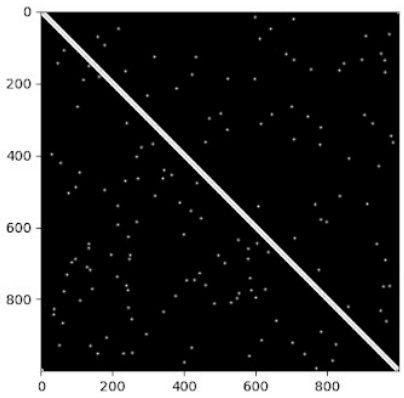

Figure 3: The network's visualized adjacency matrix, each pixel is white if the connection between the two cells indicated by the axes exists and black if it does not exist. Ultimately, the adjacency matrix was used to specify the neuronal connections in the tau propagation model.

Tau Propagation Model

Table 2: Propagation Model Parameters

Symbol	Description	Value
inhFrac	Fraction of inhibitory neurons	15%
initialFrac	Initial fraction of cells infected	0.2[a,†]
initialConc	Initial tau concentration in infected cells	0.1[a,†]
reducFactor	Tau therapeutic reduction factor	Various values[a]
prop	Proportion of infected cells impacted by therapeutic	Various values[a]
lethalThreshold	Lethal tau concentration	0.75[a]
timeSteps	Simulated time steps	20
time	Total simulated time	500 ms
dt	Time step duration	25 ms

Note. Details pertaining to all of the propagation model's parameters. [a]Values range from [0,1]. [†]Approximately models early-stage AD

Using the NEURON module in Python, each node within the network was modeled as an individual "ball and stick" neuron (one dendritic compartment and a soma) in order to simulate the morphology of neurons in early AD. The neuron's electrical behavior was represented by NEURON's conductance-based implementation.

The electrophysiological parameters of the cell included Hodgkin-Huxley dynamics with sodium, potassium, and leak currents as well as passive currents on the dendrite. The resulting spiking behavior is demonstrated in Figures 4 and 5. The cells were connected according to the adjacency matrix generated from the small-world algorithm with a mix of inhibitory and excitatory connections *inhFrac* in proportions (15% inhibitory, 85% excitatory) that are roughly similar to real cortical tissue (Swanson and Maffei, 2019).

An initial stimulation was then given to the network. This stimulation was applied to cell 500 and consisted of five simulated spikes interspaced by one millisecond.

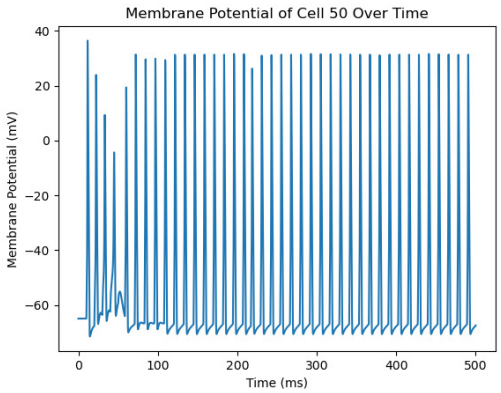

Figure 4: An example of the spiking behavior of a cell in the network.

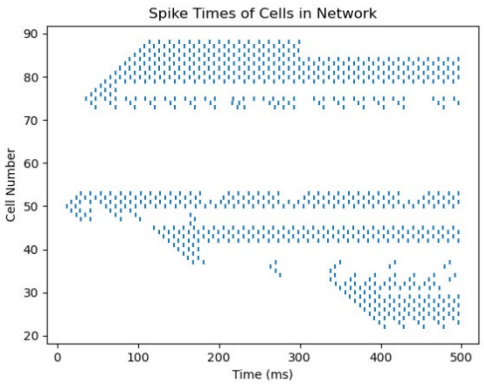

Figure 5: A raster plot describing the spike times of the cells in a 100-neuron network

Our primary novel contribution to AD research was implementing tau propagation. In the model, pathogenic tau is "seeded" by specifying a certain fraction of cells *initialFrac* which will begin the simulation with a certain concentration of pathogenic tau *initialConc*. Tau then spreads to adjacent neurons at each time step. Equation 1 was used to calculate a cell's increase in tau for a given time step. To begin calculating any given cell's gain in tau, the number of times each incident cell has fired upon it during the time step is determined. This vector of incident firing counts is divided by its sum to return a vector describing the percent firing activity for each incident neuron. Then, the change in tau is calculated as the sum of the element-wise vector multiplication of the percent firing activity vector and the vector containing the tau concentrations of each incident neuron:

$$\Delta Tau_i = \sum \left(\frac{incidentF_i}{\sum incidentF_i} \odot incidentTaus_i \right)$$

Equation 1

where *Tau* refers to the tau concentration for cell$_i$ and *incidentF* refers to the aforementioned firing counts vector. Finally, the final tau concentration of the cell is set to the sigmoid of its initial tau concentration plus the change in tau:

$$Tau_i := \sigma \left(Tau_i + \Delta Tau_i \right)$$

Equation 2

For each timestep, the procedure selects a certain proportion *prop* of infected neurons and decreases their tau concentrations by percentage *reducFactor* after the propagation. If any cell's tau concentration reaches a concentration above the lethal threshold *lethalThreshold*, that cell will be electrically disabled by changing all of its conductances to zero. This simulated apoptosis ensures that the cell can no longer fire and can not participate in the spread of tau. At each timestep, the amount of tau in each neuron is stored in a matrix. Also, the number of cells remaining alive at each timestep is tracked. The resulting time taken for one run of the simulation is about 30 minutes.

Results

When the completed model is run, the tau concentration of each cell in the network and the number of surviving cells are monitored as mentioned prior. These data are then plotted against time. An example of the graphs produced can be seen in Figures 6 and 7.

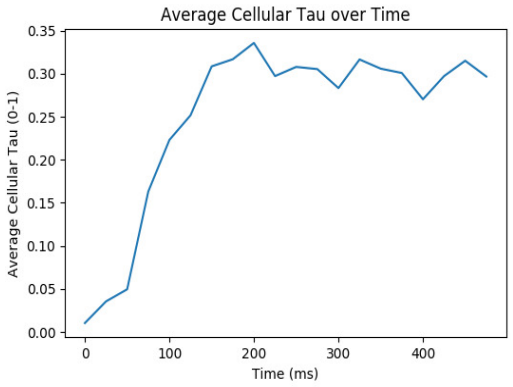

Figure 6: The average cellular tau concentration of all the cells in the network over time.

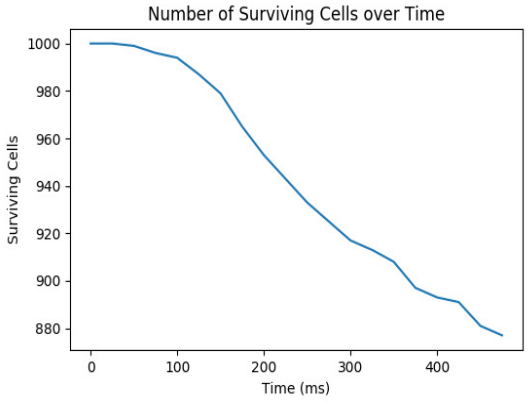

Figure 7: The number of surviving cells in the network over simulation time.

During batches of simulation runs, different values for the parameters defining the therapeutic (proportion of cells affected, tau reduction factor) were iteratively tested. The effects of varying these two parameters on the final cell survival rate at the end of the simulation is illustrated in Figure 8. For analysis purposes, each therapeutic was put into a novel class corresponding to its resulting survival rate.

Table 3: Therapeutic Classes and Survival Rates

Therapeutic Class	Resulting Neuronal Survival Rate
Class A	99-100%
Class B	95-99%
Class C	90-95%
Class D	less than 90%

Note. Each of the therapeutic classes and their corresponding survival rate ranges.

Additionally, a polynomial SVM algorithm was used to draw the decision boundaries pictured in Figure 8. The SVM was developed using Python's Scikit-learn package. This SVM algorithm can be used to predict a drug's activity class based on its reduction factor and proportion of cells affected. The SVM developed can make a prediction in about 500 milliseconds as opposed to the simulation, which

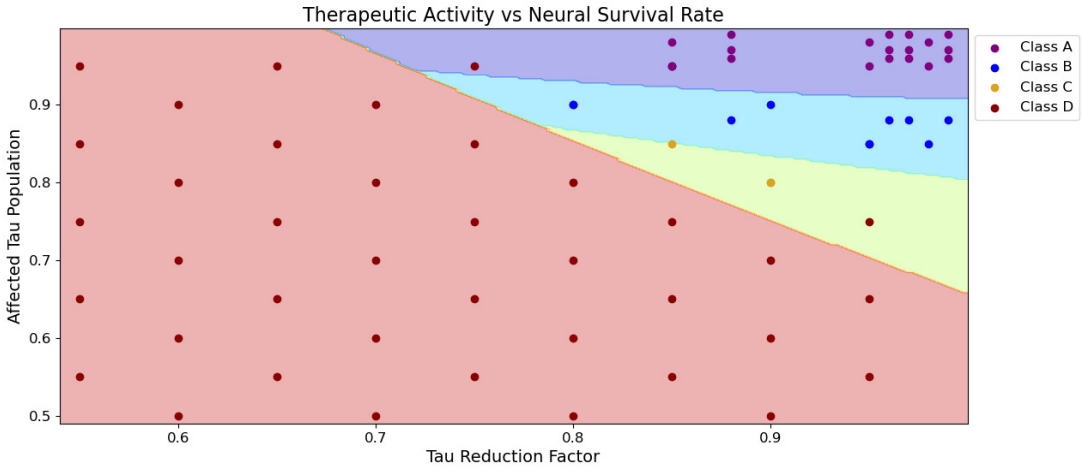

Figure 8: Each therapeutic simulated is plotted based on its reduction factor and affected proportion. The therapeutics are also color coded based upon their class as described by Table 3. The decision boundaries and background colors were drawn by the SVM classifier.

may take up to an hour to complete. The accuracy of the SVM algorithm is 95.83%. Therefore, it provides a suitable alternative to predict a drug's activity class in situations where a degree of accuracy can be sacrificed in the interest of time. However, because this SVM classifier was trained with results from running the simulation with only one set of parameters (while varying

the reduction factor and affected proportion), its results are only reliable for conditions that correspond to the other parameters listed in Table 2. To predict the class of a drug in a different set of parameters, the full simulation must be run again.

In the model, the most effective therapeutic interventions had a 99-100% survival rate (Class A therapeutics). Based on Figure 8, we hypothesized that the mean treatment population, referred to as the "affected tau population" (μP) was significantly larger than the mean tau reduction factor (μ_R) for this group. In order to test our hypothesis (H_0: $\mu_P - \mu_R = 0$, H_A: $\mu_P - \mu_R > 0$) using a two-sample t-test, all of the following conditions had to be met:

1. All data from simulations was gathered independently.
2. There was no pattern to the values (random).
3. The distributions were approximately t-shaped (Figure 9).

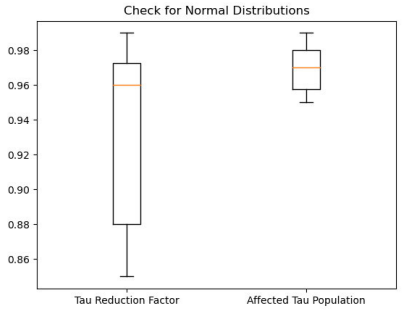

Figure 9: These box-and-whisker plots confirm that the distributions of affected tau populations and tau reduction factors were approximately t-distributions.

Next, a two-sample t-test was run with Python. The results were $t = 3.009$ and $p = 0.007$. Because the p-value was less than $\alpha = 0.01$, it could be reasonably concluded that targeting a greater tau population is more important than removing large amounts of tau for Class A therapeutics.

Also from Figure 9, it can be observed that, in order for a therapeutic to be Class A, it must have a reduction factor of at least 0.85 and an affected population of at least 0.95, suggesting that real therapeutics must have a similar effect in order to effectively halt neurodegeneration.

Varying the properties of the administered drug in the simulation allowed for drawing conclusions about what net effect a proposed drug must have in order to halt neurodegeneration. Safety of treatment and off-target effects may need to be analyzed using other computational models. As with any therapeutic, standard preclinical and clinical trials will need to take place.

Discussion

The product of this investigation is a biologically constrained model of a neuronal network through which tau propagates. The model was developed with conductance-based neurons, and (although the architecture discussed used a small-world connection) the model can accommodate virtually any connection pattern. This will allow future work to be done with the simulation that either investigates the effect of different cell types by changing electrophysiological parameters or the effect of different connection patterns on the spread of tau. This may help researchers better understand the properties of tau propagation.

Through therapeutic simulations, details regarding the characteristics of an effective intervention were uncovered. For example, the effect that varying a drug's affected population and reduction factor had on the network's final survival rate was investigated. From this, it was determined that an effective therapeutic should focus on affecting the largest fraction of infected cells, rather than reducing the tau concentrations of selected cells by a greater amount. This confirmed our first hypothesis that anti-tau therapeutics' network properties disproportionately impact therapeutic efficacy. This knowledge can be used to further direct and accelerate the process of AD drug discovery. Then, our second hypothesis, stating that an SVM algorithm could expedite the process of gauging therapeutic efficacy, was confirmed due to the aforementioned drastic time difference between running the full simulation model and the SVM.

It should be noted that the highly interconnected network structure of the brain is likely the reason that pathological tau becomes more widespread with time, rendering it harder to control (Braak and Braak, 1991; Vogel et al., 2020). Therefore, such effective therapeutics should exclusively target the transentorhinal cortex in prodromal AD (Taylor and Probst, 2008). Additionally, the future use of this model may be able to come to new conclusions about different synaptically transmissible prions, such as those involved in other neurodegenerative disorders.

Despite our considerations, there are a few limitations in the design that should be addressed. First, the proposed model only depicts one isoform of tau and assumes that synaptic transmission is the only significant manner in which tau can spread. As a result, effects of the polymerization of tau, its passive leakage from degenerated cells, as well as residual tau from dead cells (ghost tangles) are not considered by the model (Colin et al., 2020). Other factors were omitted, including the side effects from tau overexpression and presence of glial cells (Colin et al., 2020; Vogel et al., 2020). Additionally, the assumption was made that the simple "ball and stick" neurons would act as sufficiently accurate neurons for the purpose of the simulation. Simplifying the neuron's morphological and electrophysical properties was a necessary sacrifice, as simulating a network of 1000 physiologically accurate neurons would take substantially more computation time. However, because only the firing rates of the cells were measured, these simplifications should have had little effect on the final results. Additionally, the simulation could have benefited from running in parallel rather than serial, as this should improve its performance.

Another limitation involved the exclusive focus on tau pathology, independent of the protein amyloid-β, which congregates in the extracellular space and forms amyloid plaques, which can also contribute to AD pathology (Ramirez-Bermudez, 2012). Tau protein has been shown to interact with aberrant amyloid-β in a positive feedback loop (Leroy et al., 2012). Future research should consider this interaction by modifying the model.

Several other directions are possible for future research. In our model, a random small-world network was created. In the future, the biological relevance could be enhanced by using experimental data to further constrain the connectivity of the model. Experimentalists can use novel technology such as an automatic tape-collecting ultramicrotome to retrieve brain sections cut along a continuous submerged conveyor belt (Kasthuri et al., 2015). Then, thinly sliced brain sections can be visualized using electron microscopy and converted into voxels in a database (Kasthuri et al., 2015). These voxels could eventually replace the small-world network architecture by providing a more accurate map of cortical connections, in turn yielding better results. Moreover, detailed cortical data will make another analysis possible: graph theory research can pinpoint hub cells which are characterized by either high convergence (number of inputs) or divergence (number of outputs) (Watts and Strogatz, 1998; Van et al., 2013). Therapeutic intervention in the model can then be localized to target hub cells, which will have a larger impact on net tau propagation in a neuronal network. This may be instrumental in developing novel targeted therapeutics for AD.

Because our model solely takes parameters for protein removal, its use is not limited to pharmaceutical therapeutics. There have been biomedical engineering efforts to physically remove amyloid plaques by introducing nanoparticles that cross the blood-brain barrier and apply localized magnetic fields (Ahmad et al., 2017). In this design, modified antibodies against amyloid-β act as "sensors" and reduce off-target effects (Ahmad et al., 2017). The same mechanism can likely be applied to extracellular tau, but the antibodies will detect harmful tau protein isoforms instead of amyloid-β. Moreover, tau pathology may be treatable with noninvasive gamma waves (Iaccarino et al, 2016). Since 40 Hz gamma oscillations facilitate working memory, they can simultaneously be used to treat AD symptoms of dementia and stop tau propagation (Rochart et al., 2020). All of these techniques can be analyzed for efficacy within our model.

In summary, our model has the potential to aid in the future development of tau-based AD therapeutics by explaining what characteristics of

proposed therapeutics are most predictive of high efficacy. The model is also highly adaptable, making it useful to study other prion-related disorders or types of therapeutics with minimal modification.

Acknowledgements

We would like to thank Kaitlyn Dorst, Scott Knudstrup, and the rest of the Boston University RISE staff for their unconditional support and guidance during our research.

Corresponding Author

Marianne Bezaire
Boston University
mbezaire@bu.edu
610 Commonwealth Avenue Rm. 723B, Boston, MA 02215

Supplementary Information

Code Repository:
https://github.com/BashirSbaiti/TauPropagationModel

References

Adams, S. J., DeTure, M. A., McBride, M., Dickson, D. W., & Petrucelli, L. (2010). Three repeat isoforms of tau inhibit assembly of four repeat tau filaments. PloS one, 5(5), e10810.

Ahmad J, Akhter S, Rizwanullah M, Khan MA, Pigeon L, Addo RT, Greig NH, Midoux P, Pichon C, Kamal MA (2017) Nanotechnology Based Theranostic Approaches in Alzheimer's Disease Management: Current Status and Future Perspective. Curr Alzheimer Res 14:1164–1181.

Alzheimer's Association (2019) 2019 Alzheimer's disease facts and figures. Alzheimer's Dement 15:321–387. Available at: https://alz-journals.onlinelibrary.wiley.com/doi/abs/10.1016/j.jalz.2019.01.010.

Alzheimer's Association (2021) 2021 Alzheimer's disease facts and figures. Alzheimer's Dement 2021:17(3). Available at: https://www.alz.org/media/documents/alzheimers-facts-and-figures.pdf

Braak H, Braak E (1991) Neuropathological stageing of Alzheimer-related changes. Acta Neuropathol 82:239–259.

Braak H, Braak E (1995) Staging of Alzheimer's disease-related neurofibrillary changes. Neurobiol Aging 16:271–278.

Colin M, Dujardin S, Schraen-Maschke S, Meno-Tetang G, Duyckaerts C, Courade J-P, Buée L (2020) From the prion-like propagation hypothesis to therapeutic strategies of anti-tau immunotherapy. Acta Neuropathol 139:3–25 Available at: https://doi.org/10.1007/s00401-019-02087-9.

Cortes-Canteli, M., & Iadecola, C. (2020). Alzheimer's disease and vascular aging: JACC focus seminar. Journal of the American College of Cardiology, 75(8), 942-951.

Courade JP et al. (2018) Epitope determines efficacy of therapeutic anti-Tau antibodies in a functional assay with human Alzheimer Tau. Acta Neuropathol 136:729–745 Available at: https://doi.org/10.1007/s00401-018-1911-2.

Frost B, Jacks RL, Diamond MI (2009) Propagation of Tau misfolding from the outside to the inside of a cell. J Biol Chem 284:12845–12852.

Hyman BT (1997) The neuropathological diagnosis of Alzheimer's disease: Clinical-pathological studies. Neurobiol Aging 18:S27–S32.

Iaccarino HF, Singer AC, Martorell AJ, Rudenko A, Gao F, Gillingham TZ, Mathys H, Seo J, Kritskiy O, Abdurrob F, Adaikkan C, Canter RG, Rueda R, Brown EN, Boyden ES, Tsai LH (2016) Gamma frequency entrainment attenuates amyloid load and modifies microglia. Nature 540:230–235.

Iqbal, K., Liu, F., Gong, C. X., & Grundke-Iqbal, I. (2010). Tau in Alzheimer disease and related tauopathies. Current Alzheimer Research, 7(8), 656-664.

Iqbal K, Zaidi T, Wen GY, Grundke-Iqbal I, Merz PA, Shaikh SS, Wisniewski HM,

Alafuzoff I, Winblad B (1986) Defective brain microtubule assembly in Alzheimer's disease. Lancet 328:421–426.

Kasthuri N et al. (2015) Saturated Reconstruction of a Volume of Neocortex. Cell 162:648–661.

Leroy, K., Ando, K., Laporte, V., Dedecker, R., Suain, V., Authelet, M., ... & Brion, J. P. (2012). Lack of tau proteins rescues neuronal cell death and decreases amyloidogenic processing of APP in APP/PS1 mice. The American journal of pathology, 181(6), 1928-1940.

Luna-Munoz, J., Chavez-Macias, L., Garcia-Sierra, F. and Mena, R., 2007. Earliest Stages of Tau Conformational Changes are Related to the Appearance of a Sequence of Specific Phospho-Dependent Tau Epitopes in Alzheimer's Disease 1. Journal of Alzheimer's Disease, 12(4), pp.365-375.

Nicholls SB, Devos SL, Commins C, Nobuhara C, Bennett RE, Corjuc DL, Maury E, Eftekharzadeh B, Akingbade O, Fan Z, Roe AD, Takeda S, Wegmann S, Hyman BT (2017) Characterization of TauC3 antibody and demonstration of its potential to block tau propagation. PLoS One 12 Available at: https://doi.org/10.1371/journal.pone.017791.

Noble, W. S. (2006). What is a support vector machine?. Nature biotechnology, 24(12), 1565-1567.

Nobuhara CK et al. (2017) Tau Antibody Targeting Pathological Species Blocks Neuronal Uptake and Interneuron Propagation of Tau in Vitro. Am J Pathol 187:1399–1412.

Pisner, D. A., & Schnyer, D. M. (2020). Support vector machine. In Machine Learning (pp. 101-121). Academic Press.

Ramirez-Bermudez J (2012) Alzheimer's Disease: Critical Notes on the History of a Medical Concept. Arch Med Res 43:595–599.

Rochart R, Liu Q, Fonteh AN, Harrington MG, Arakaki X (2020) Compromised Behavior and Gamma Power During Working Memory in Cognitively Healthy Individuals With Abnormal CSF Amyloid/Tau. Front Aging Neurosci 12:339 Available at: https://www.frontiersin.org/article/10.3389/fnagi.2020.574214.

Serrano-Pozo A, Frosch MP, Masliah E, Hyman BT (2011) Neuropathological alterations in Alzheimer disease. Cold Spring Harb Perspect Med 1 Available at: http://perspectivesinmedicine.cshlp.org/.

Stopschinski BE, Diamond MI (2017) The prion model for progression and diversity of neurodegenerative diseases. Lancet Neurol 16:323–332.

Swanson OK, Maffei A (2019) From hiring to firing: Activation of inhibitory neurons and their recruitment in behavior. Front Mol Neurosci 12 Available at: www.frontiersin.org.

Takeda S (2019) Tau Propagation as a Diagnostic and Therapeutic Target for Dementia: Potentials and Unanswered Questions. Front Neurosci 13 Available at: www.frontiersin.org.

Taylor, K. I., & Probst, A. (2008). Anatomic localization of the transentorhinal region of the perirhinal cortex. Neurobiology of aging, 29(10), 1591-1596.

Van den Heuvel MP, Sporns O (2013) Network hubs in the human brain. Trends Cogn Sci 17:683–696 Available at: http://dx.doi.org/10.1016/j.tics.2013.09.012.

Vishwanathan, S. V. M., & Murty, M. N. (2002, May). SSVM: a simple SVM algorithm. In Proceedings of the 2002 International Joint Conference on Neural Networks. IJCNN'02 (Cat. No. 02CH37290) (Vol. 3, pp. 2393-2398). IEEE.

Vogel JW, Iturria-Medina Y, Strandberg OT, Smith R, Levitis E, Evans AC, Hansson O (2020) Spread of pathological tau proteins through communicating neurons in human Alzheimer's disease. Nat Commun 11:2612 Available at: https://doi.org/10.1038/s41467-020-15701-2.

Wang Y, Balaji V, Kaniyappan S, Krüger L, Irsen S, Tepper K, Chandupatla R, Maetzler W, Schneider A, Mandelkow E, Mandelkow E-M (2017) The release and trans-synaptic transmission of Tau via exosomes. Mol Neurodegener 12:5 Available at: https://doi.org/10.1186/s13024-016-0143-y.

Warren, C. P., Sander, L. M., & Sokolov, I. M. (2002). Geography in a scale-free network model. Physical Review E, 66(5), 056105.

Watts DJ, Strogatz SH (1998) Collective dynamics of "small-world" networks. Nature 393:440–442.

Watts DJ (2018) Small Worlds: The Dynamics of Networks between Order and Randomness. Princeton University Press. Available at: https://doi.org/10.1515/9780691188331.

Williams DR (2006) Tauopathies: classification and clinical update on neurodegenerative diseases associated with micro tubule-associated protein tau. Intern Med J 36:652–660.

Yamada K, Holth JK, Liao F, Stewart FR, Mahan TE, Jiang H, Cirrito JR, Patel TK, Hochgräfe K, Mandelkow E-M, Holtzman DM (2014) Neuronal activity regulates extracellular tau in vivo. J Exp Med 211:387–393 Available at: https://doi.org/10.1084/jem.20131685.